A transfer Bayesian learning methodology for SHM of monumental structures

Laura Ierimonti[a,*], Nicola Cavalagli[a], Ilaria Venanzi[a], Enrique García-Macías[a], Filippo Ubertini[a]

[a]*Department of Civil and Environmental Engineering, University of Perugia. Via G. Duranti, 93 - 06125 Perugia, Italy.*

Abstract

A critical aspect related to the damage detection strategies by using structural health monitoring (SHM) is the lack of diagnostic labels able to assign a damage class to the measured data. In this context, a semi-supervised learning methodology, designated as transfer Bayesian learning (TBL), is proposed with the main objective of labeling post-processed data by selecting a limited number of informative elements. The method suggested in this work allows to define multi-class labels by making use of a digital twin (DT) of the structure, as a function of specific damage-sensitive mechanical parameters. The methodology is applied in a monumental building, the Consoli Palace, located in Gubbio, central Italy. The structure is instrumented with several sensors in order to measure vibrations, temperature and possible variation of existing cracks' amplitudes. Several nonlinear pushover analyses are carried out on a calibrated finite element (FE) model to use them in conjunction with Engineering judgment for the definition of the damage-sensitive areas. The DT is then used as class classifier by means of a sensitivity damage chart (SDC). Finally, a Bayesian model updating of the damage-dependent parameters allows the probabilistic

*Corresponding author. Department of Civil and Environmental Engineering, University of Perugia. Via G. Duranti, 93 - 06125 Perugia, Italy. phone: +39 075 585 3908; fax: +39 075 585 3897.

Email addresses: laura.ierimonti@unipg.it (Laura Ierimonti), nicola.cavalagli@unipg.it (Nicola Cavalagli), ilaria.venanzi@unipg.it (Ilaria Venanzi), enrique.garciamacias@unipg.it (Enrique García-Macías), filippo.ubertini@unipg.it (Filippo Ubertini)

damage detection and identification.

Keywords: Transfer learning, Bayesian model updating, digital twin, damage classification, continuous monitoring

---

Nomenclature

α	Kriging approximation error
β	Kriging regression parameters
$\hat{y}$	Kriging predictor
$\mathbf{X}$	Design parameters
$\mathbf{x}$	SSI-based state vector
$\mathbf{Y}$	Observation vector
$\mathbf{Y}$	Vector collecting parameters of the FE model to be calibrated
$\mathbf{y}$	SSI-based vector of output measurements
$\mathcal{M}$	FE model
$\mathcal{S}$	Design sets
$\mathscr{F}$	Kriging regression model
$\mathscr{M}$	Mathematical model
$\mathscr{R}$	Kriging correlation matrix
$\overline{k}_j$	Damage threshold k_j
Φ	Mode shape
σ	Standard deviation
$\mathbf{A}$	SSI-based system matrix

$\mathbf{C}$	SSI-based output matrix
$\mathbf{v}$	SSI-based vector of noise of measurements
$\mathbf{w}$	SSI-based vector of external input
θ	Kriging correlation parameters
ζ	Damping coefficient
c	Bayesian normalizing factor
D	Total number of measured data
d	Measured data
f	Frequency
$F(\cdot)$	Standard Gaussian cumulative distribution function
i	Index of natural vibration mode
J	Objective function
j	Index of design parameters to be updated
J^{err}	Bayesian error function
k_j	multiplying coefficients of x_j
M	Total number of vibration modes
m	Index of measured data
N	Total number of x_j design parameters to be updated
N_s	Number of samples
p	Probability density function
P_j^{al}	Alarm function
P_j^{dam}	Damage probability

p_1, p_2	Weights of objective function
r	Kriging correlation components of $\mathscr{R}$
R^2	Coefficient of determination
T	Dimension of training population
t	Time
U	Total no. of FE uncertain parameters to be
up	Updtaed
cov	Covariance
DT	Digital Twin
MF	Modal Features
ref	Undamaged reference state
SDC	Sensitivity Damage Chart
TBL	Transfer Bayesian Learning
TL	Transfer Learning

1. Introduction

Structural damages suffered by monumental structures during recent earthquakes have gained attention on SHM-based damage detection and localization methodologies, due to the low economic impact and non-destructive nature of SHM technology [1]. Indeed, continuous SHM can accomplish the complex task of ensuring risk reduction in regions characterized by a relevant cultural heritage like Italy, which has the greatest number of UNESCO world heritage sites in the world [2].

Different works in literature make use of SHM as a powerful tool for investigating the evolution with time of the structural modal parameters which are

related to material's damage and deterioration [3, 4, 5, 6] and for investigation of the dynamic behavior of masonry bell towers [7, 8, 9, 10, 11]. Since relevant variations in the dynamic response of an healthy structure can also be related to changes in the environmental conditions, many works are devoted to the study of proper techniques able to remove the effects of temperature and humidity [12, 13]. The use of surrogate models, i.e. DT, for handling uncertainties in SHM is explored in [14, 15]. Recently, the benefits of SHM were widely exploited in literature for bridges [16, 17, 18, 19] and a brief review on SHM for data-driven damage identification problems is given in [20].

SHM is also explored in literature for damage assessment by means of Bayesian model updating, in order to deal with different sources of uncertainty [21]. On the one hand, the use of an updated FE model to reach an accurate response prediction of the real structure is widely investigated in literature [22, 23, 24, 25, 26, 27], since a Bayesian statistical framework is able to handle the inherent ill-conditioning and possible non-uniqueness in model updating processes [28, 29]. On the other hand, only a few recent contributions deal with long-term SHM data and damage detection. In particular, Behmanesh et al. [30, 31] proposed a model updating technique based on hierarchical Bayesian modeling for identification of civil structural systems under changing environmental conditions accounting for different subgroups of measured data, while Sun et al. [32] adopted a hierarchical Bayesian framework with Laplace priors for updating the finite element model. An iterative procedure for damage detection and localization by using the Bayesian framework through the Transitional Markov Chain Monte Carlo (TMCMC) is proposed in [33]. A Bayesian model updating framework of an historic masonry tower is developed in [34], while in [35] a Bayesian-based technique is used for the updating of the mechanical properties associated to the base isolation system installed on a school building.

As confirmed by the literature on the topic presented above, nowadays the most common procedure in civil SHM concerns the data acquisition and feature extraction (system eigenfrequencies and modal shapes) through signal processing [36, 37]. Then, a smart statistical classification is necessary to convert

monitoring data into damage information, improving the accuracy of predictive models. This task could be accomplished by exploiting machine learning (ML) techniques, which can be divided in three main categories: supervised learning, unsupervised learning, semi-supervised learning. In the supervised learning paradigm, monitoring data can be associated with known labeled features that define the meaning of data. Conversely, in the unsupervised learning paradigm the problem is characterized by a massive amount of unlabeled data. At the intermediate level, semi-supervised learning allows the use of data with and without descriptive labels, which is more feasible in the context of SHM damage identification. Indeed, damage identification problems can be recognized as a five-level hierarchical approach [36]: (i) detection; (ii) localization; (iii) classification ; (iv) assessment; (v) prediction. Conventional SHM-systems can be classified as unsupervised learning, since they typically allow to capture modifications of the global behavior (i) of the structure (novelty detection).

Over the last decades, the concepts of ML have been approaching the SHM field [38, 39, 18]. A probabilistic framework for the classification, investigation and labelling of data is suggested in [40] and a semi-supervised Gaussian mixture model for a probabilistic damage-classification is presented in [41].

Considering the literature background, a big effort still needs to be done to develop an automated SHM- and model-based damage detection framework considering at the same time: robustness, accuracy and long-term data.

Since model-based approaches are typically ill-conditioned, some priority needs to be made to cleverly label the data. The process of prioritizing monitored data by using the numerical model fits into the transfer learning (TL) technique, a semi-supervised learning approach where the learning algorithm is allowed to build a labeled training set autonomously [42, 36, 43].

In this context, this paper presents a TBL methodology based on long-term monitoring data aimed at evaluating the possible damage of monumental structures, where TL concepts allow to mitigate the shortage of labeled structural data and a trained DT is used as a formal prior belief for damage assessment. The idea is that it is possible to learn relationships from data. In the context of

SHM, this means that it is possible to assign a damage state or class by using a trained numerical model in order to detect damage at the earliest possible time and in an automatic manner. Then, a Bayesian-based procedure allows to trace over time the probability of occurrence of possible damage scenarios.

The case study is the Consoli palace located in Gubbio, near Perugia, in Italy, a complex historical masonry buildings. The structure has been monitored by the Authors since 2015 and the SHM sensors' network has been enhanced in 2020. The continuous monitoring data are used for the Bayesian-based updating of specific mechanical properties of some portions of the structure, identified as the most damage-sensitive ones by means of non-linear static analyisis (NLSA) and Engineering judgment. The prior knowledge of the uncertain parameters is sequentially updated on the basis of a trained DT consisting of a surrogate model. Probabilistic damage identification is performed by using the SDC, i.e., a graphical chart able to associate to the frequencies decay a stiffness reduction, which is a possible sign of damage. The effectiveness of the proposed methodology is demonstrated by the numerical simulation of a feasible damage scenario. The results show the advantage of having long-term monitoring data on the correct estimation of the uncertain parameters' distribution. The main advantages and innovations of the proposed approach can be summarized as follows: i) the availability of a big amount of long-term monitoring data allows to timely estimate the trend of uncertain parameters, i.e., distinguishing variations due to changes in environmental conditions (which can be removed by means of regression models) from damage/deterioration over time; ii) the subsequent updating of the damage-sensitive uncertain parameters triggers the robust identification of possible damage scenarios; iii) the use of a digital twin allows to overcome the shortage of labeled structural data and to transfer knowledge between numerical models and online monitoring data; iv) the results are periodically updated in terms of damage probabilities, which allow an essential support for decision making; v) once the model is trained, the methodology is computationally efficient, allowing the rapid diagnosis and damage localization.

The rest of the paper is organized as follows. Section 2 presents the proposed

methodology for continuous SHM and Bayesian model updating. Section 3 describes the monumental building selected as case study, the continuous monitoring system and the FE model. Section 4 illustrates the results and, finally, Section 5 concludes the paper.

2. The proposed TBL methodology

The proposed methodology, schematically represented in Fig. 1, embraces different consequential steps which can be summarized as follows:

1. Data acquisition from the monitoring system which typically consists of acceleration data, temperature information and static measurements, such as crack amplitudes.

2. Continuous post-processing over time in order to estimate the modal features (MF), i.e., natural frequencies f_i^{exp}, mode shapes $\boldsymbol{\Phi}_i^{\text{exp}}$ and damping coefficients ζ_i^{exp} associated with the i^{th} natural vibration mode from operational vibration measurements.

3. If t=1; t denoting discrete time (days):
   i) Preliminary FE modeling and evaluation of damage-sensitive portions on the basis of NLSA and Engineering judgment.
   ii) Calibration of the digital twin as a function of the uncertain parameters to be updated associated to each damage-sensitive portion.
   iii) Damage classification in order to construct the SDC, i.e., a graphical chart able to associate a stiffness reduction to the frequencies decay for the selected damage scenarios.

4. if t >1:
   i) Novelty detection on a daily basis t, i.e. daily average values of MF. If a novelty is detected, increase the frequency of the modal tests on a hourly basis $t = t^*$, i.e., MF(t^*).

ii) Perform the Bayesian model updating of the uncertain parameters by means of the SDC.

iii) Assign a damage probability for damage identification.

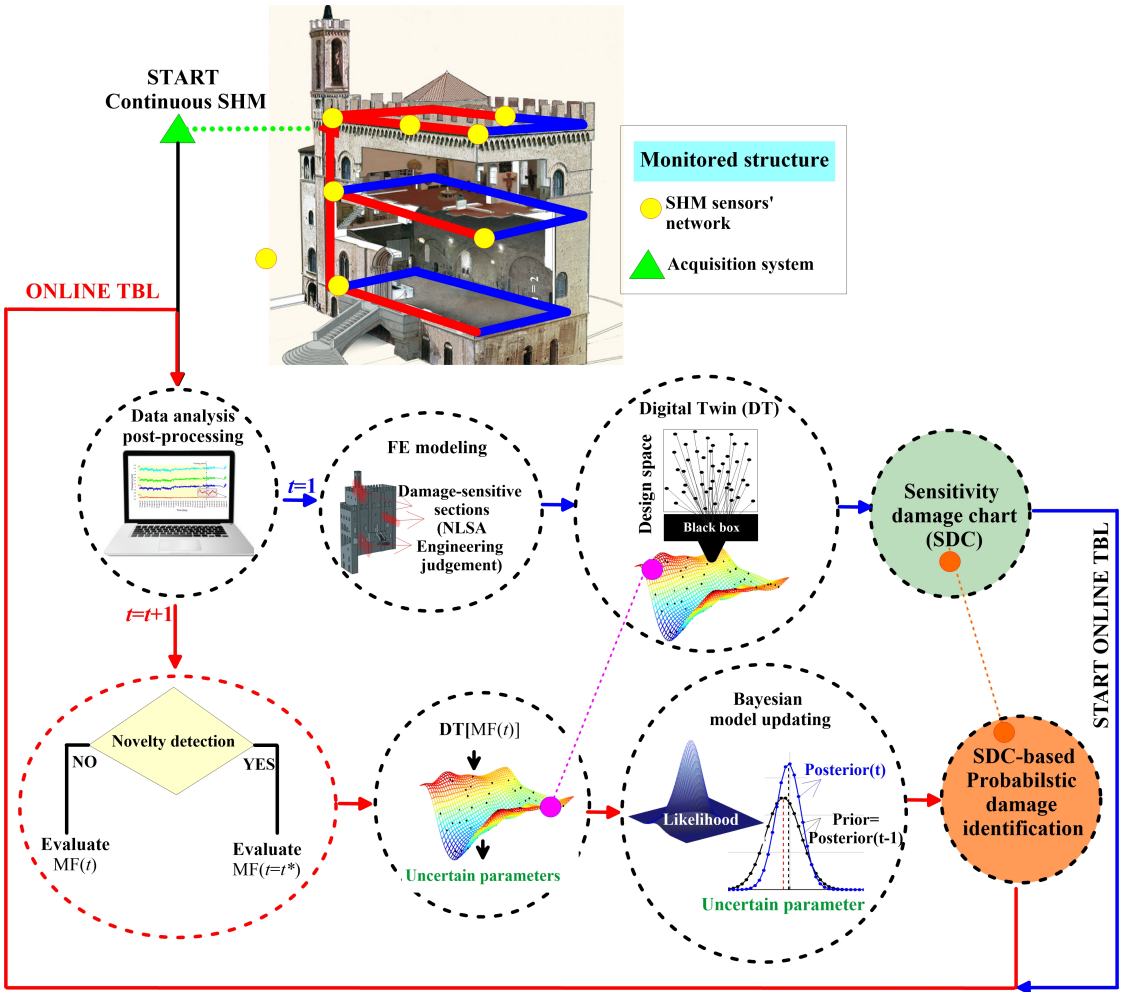

Figure 1: The proposed TBL methodology.

The main advantage of the proposed methodology is the possibility to evaluate in a timely and continuous manner any MF variation in the structure which is commonly considered as a sign of possible damage [4]. Then, the use of the SDC, numerically reconstructed from the DT, allows to detect damage with a

probabilistic approach.

The consequential steps of the proposed methodology are detailed in the following subsections.

2.1. Data acquisition and post-processing

In order to continuously investigate over time the MF, it is convenient to optimize the sensors' placement scheme across the structure and levels, connecting the sensors to one single centralized acquisition system.

Then, vibration data are timely converted into modal properties (data post-processing) through the MOSS integrated software [44] by means of an automated covariance-based stochastic subspace identification (SSI) technique [17]. More in depth, a SSI-based algorithm identifies a stochastic state-space model whose mathematical formulation can be expressed as:

$$\begin{aligned} \mathbf{x}_{t+1} &= \mathbf{A}\mathbf{x}_t + \mathbf{w}_t \\ \mathbf{y}_t &= \mathbf{C}\mathbf{x}_t + \mathbf{v}_t \end{aligned} \tag{1}$$

in which t is the time step, $\mathbf{x} \in \mathbb{R}^{q\times 1}$ is the state vector (with q order of the identified model), $\mathbf{y} \in \mathbb{R}^{L\times 1}$ is the vector collecting the L output measurements, $\mathbf{A} \in \mathbb{R}^{q\times q}$ is the system matrix storing modal information, $\mathbf{C} \in \mathbb{R}^{L\times q}$ is the corresponding output matrix, $\mathbf{w} \in \mathbb{R}^{q\times 1}$ and $\mathbf{v} \in \mathbb{R}^{L\times 1}$ are white noise vectors, considered as zero-mean stochastic processes and independent of the state vector, representing the external input and the noise of the measurements, respectively. Then, by a complex transformation of the state-space system rewritten in frequency domain by its transfer function, the modal features can be extracted. Environmental effects should be removed from original signals on the basis of a selected training period. In order to distinguish variations due to environmental conditions from possible damages, different statistical models can be adopted. In the proposed methodology, the least-angle regression (LAR) algorithm is used for fitting linear regression models.Add reference and a small part describing the LAR algorithm (ENRIQUE).

2.2. Preliminary FE modeling

This step consists of building a numerical model $\mathcal{M}$ of the structure on the basis of in-situ inspections and available documents as structural drawings. At this stage, a series of assumptions mus typically be made regarding boundary conditions, material properties, mechanical characteristics and more.

In order to simulate the dynamic behavior of the structure and the damage process, it is necessary to calibrate the FE model $\mathcal{M}$.

The calibration process is usually formulated as an optimization problem whereby some physical/mechanical parameters of the structure are adjusted to minimize the gap between numerical and experimental modal characteristics. The calibration process can be summarized as follows:

1. identify the structural modal parameters, i.e., the frequency f_i^{exp} and the mode $\mathbf{\Phi}_i^{\text{exp}}$ associated to the i^{th} natural vibration mode, via ambient vibration tests (AVT);
2. create an initial FE model of the structure on the basis of data obtained from available technical documents and/or in-situ inspections and define the vector $\mathbf{Y} = \{\mathbf{Y}_1, .., \mathbf{Y}_u, .., \mathbf{Y}_U\}$ collecting parameters to be calibrated (for instance $\mathbf{Y}_u$ is the vector collecting Young's modulus E, shear modulus G, Poisson's ratio ν and mass density w);
3. perform a preliminary modal analysis and evaluate the i^{th} numerical natural frequency f_i^{FEM} and vibration mode $\mathbf{\Phi}_i^{\text{FEM}}$;
4. calculate the optimum values $\mathbf{Y}^{\text{opt}}$ via optimization problem:

$$\mathbf{Y}^{\text{opt}} = \arg\min_{Y \in \mathfrak{D}} J(\mathbf{Y}) \tag{2}$$

where the objective function $J(\mathbf{X})$ is defined as:

$$J(\mathbf{Y}) = \sum_{i=1}^{M} p_1 \eta_{f,i}(\mathbf{X}) + p_2 \eta_{\Phi,i}(\mathbf{Y}) \tag{3}$$

with

$$\eta_{f,i}(\mathbf{Y}) = \frac{\left| f_i^{\text{exp}} - f_i^{\text{FEM}} \right|}{f_i^{\text{exp}}},\ \eta_{\mathbf{\Phi},i}(\mathbf{Y}) = 1 - \text{MAC}_i(\mathbf{Y}) \tag{4}$$

where M is the number of vibration modes; MAC_i denotes the Modal Assurance Criterion (MAC) between the i^{th} experimental $\mathbf{\Phi}^{\mathrm{exp}}$ and numerical $\mathbf{\Phi}^{\mathrm{FEM}}$ mode shapes, while p_1 and p_2 represent the weights of the objective function.

Once the model is calibrated, different damage scenarios can be simulated through both Engineering judgment and nonlinear static analyses (NLSA). As a result, the definition of damage scenarios allows to isolate the elements which are more prone to damage and select them into different regions $\mathcal{R} = \{\mathcal{R}_1, .., \mathcal{R}_j, .., \mathcal{R}_N\}$, where N is the total number of design sets. At this point, the jth region can be used as an homogeneous portion of the structure in terms of material's stiffness and the vector $\mathbf{X}(\mathcal{R}) = \{k_1(\mathcal{R}_1), .., k_j(\mathcal{R}_j), .., k_N(\mathcal{R}_N)\}$ collecting the multiplier of the Young moduli (k_j) of all the elements comprises in that region, with $0 \leq k_j \leq 1$. For the sake of simplicity, the dependence on $\mathcal{R}$ in the term $\mathbf{X}(\mathcal{R})$ is dropped hereafter.

2.3. Sensitivity damage chart: DT modeling

In order to perform the model-based process of damage classification within the TL framework in a computationally-effective manner given E_N damage-sensitive parameters, a numerical DT needs to be trained, i.e., a input/output black box model as represented in Fig. 2. Once a training population for vector

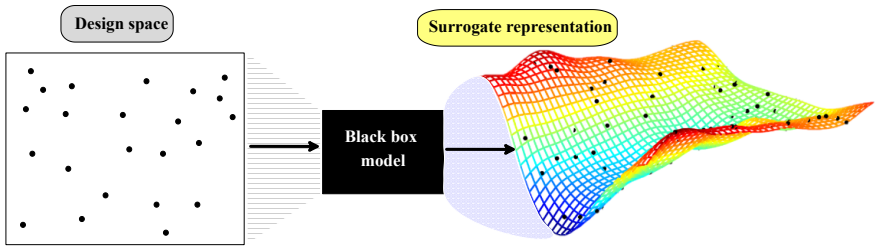

Figure 2: A schematic representation of the DT model numerical reconstruction.

$\mathbf{X}$ is selected, it is possible to get the predictions of the black box model as a

function of the model type (linear model, quadratic model, etc). Then, in order to measure how well the defined DT replicates the predictions of the black box model, the coefficient of determination R^2 can be evaluated [45]:

$$R^2 = 1 - \frac{\sum_T \left(y_T^* - y_T\right)^2}{\sum_T \left(y_T - \overline{y}\right)^2} \tag{5}$$

where T is the dimension of the training population; y_T^* is the prediction for the T^{th} instance of the surrogate model, y_T is the prediction of the black box model and $\overline{y}$ is the mean of the black box model predictions.

The R^2 represents the percentage of variance that is captured by the surrogate model. Indeed, if R^2 is close to 1 means that the model well approximates the behavior the black box model very well, while if R^2 approaches 0 the model fails.

For the present application, the Kriging-based DT model, which is the most commonly used in geostatistical approach for spatial interpolation [14], is applied.

The Kriging interpolator is based on statistical models and is capable of reproducing a prediction surface with a certain accuracy. According to this method, the process that originates the data $y(\mathbf{X})$ can be divided into a regression model $\mathscr{F}$, i.e., the deterministic component, and an approximation error α, i.e., the stochastic component [46]:

$$y(\mathbf{X}) = \mathscr{F}(\boldsymbol{\beta}, \mathbf{X}) + \alpha(\mathbf{X}) \tag{6}$$

where $\boldsymbol{\beta}$ are the regression parameters of $\mathscr{F}$ which can be defined as a linear combination of p selected functions $\mathrm{f}_i : \mathbb{R}^N \to \mathbb{R}$:

$$\mathscr{F}(\boldsymbol{\beta}, \mathbf{X}) = \beta_1 \mathrm{f}_1(\mathbf{X}) + ... + \beta_p \mathrm{f}_p(\mathbf{X}) = F(\mathbf{X})^T \boldsymbol{\beta} \tag{7}$$

The approximation error α is assumed as a random process with zero mean and covariance $\mathrm{cov}(X_i, X_j) = \sigma^2 \mathscr{R}\big(\theta, X_i, X_j\big)$, with σ^2 variance of $\mathscr{F}(\boldsymbol{\beta}, \mathbf{X})$ and $\mathscr{R}$ the matrix of stochastic-process correlations with components $r\big(\theta, X_i, X_j\big)$, θ

being the correlation parameters. Then, considering an arbitrary point $\mathbf{X}$, the Kriging predictor can be defined as follows:

$$\hat{y}(\Theta) = F(\mathbf{X})^T \boldsymbol{\beta} + r(\mathbf{X})^T \gamma^* \tag{8}$$

where $\gamma^* = \mathscr{R}^{-1}[Y - F(\mathbf{X})^T \boldsymbol{\beta}]$ and $r(\mathbf{X}) = [r\big(\theta, X_1, X\big), ..., r\big(\theta, X_N, X\big)]$. It is important to note that for a fixed set of design data, β and γ^* are fixed. Therefore, the Kriging model can be numerically reconstructed by selecting the regression and the correlation models. The Kriging model is then used as a classification DT model for the damage and the SDC is built, which allows to define a correlation between the design scenarios and the experimentally measured modal characteristics in terms of frequency decays and MAC modification. Hence, the sensitivity damage chart can be considered the core of the TBL. Given the assumption that the DT can suitably represent the structural behavior in the neighborhood of the initial values of the uncertain parameters, the calibration of the surrogate model can be dropped for $t > 1$.

2.4. The Bayesian-based FE model updating

The Bayesian model updating at time t consists of evaluating the posterior probability density function $p(\mathbf{X}\big|\mathbf{d}, t, \mathscr{M})$ of the uncertain parameters to be updated $\mathbf{X}$ conditional on a set of measured data $\mathbf{d}(t)$ of the system and a selected mathematical model $\mathscr{M}$ by using the likelihood of measured data and the prior knowledge acquired at $t-1$. In mathematical terms, Bayes' theorem gives:

$$p(\mathbf{X}\big|\mathbf{d}, t, \mathscr{M}) = c \cdot p(\mathbf{d}\big|\mathbf{X}, t, \mathscr{M}) \cdot p(\mathbf{X}\big|t, \mathscr{M}) \tag{9}$$

where $\mathbf{X} = \{k_1, .., k_N\}$ is the vector collecting the N adjustable damage-sensitive parameters; $c = 1/\int p(\mathbf{d}\big|\mathbf{X}, t, \mathscr{M}) p(\mathbf{X}\big|\mathscr{M}) \mathrm{d}\mathbf{X}$ is a normalizing factor called the evidence of the model class $\mathscr{M}$, which ensures that the posterior distribution integrates to one; $p(\mathbf{d}\big|\mathbf{X}, t, \mathscr{M})$ is the likelihood function which gives

a measure of the agreement between the measured data $\mathbf{d}$ and the predicted data $\mathbf{X}$; $p(\mathbf{X}|t, \mathscr{M})$ is the prior probability density function (PDF) of $\mathbf{X}$ evaluated as the posterior distribution at $t-1$, i.e., $p(\mathbf{X}|\mathbf{d}, t-1, \mathscr{M})$. For the sake of clarity, since only one FE model is used in the analysis, the reference mathematical model $\mathscr{M}$ is dropped hereafter.

In a continuous online monitoring process, many data sets are available for the Bayesian model updating. Hence, the prior distribution, winch has the main role of regulator of the Bayesian-based process, becomes more informative and strongly biased as the number of data increases, getting barely persuaded by a possible damage occurrence. Therefore, so many additional damage-based data can overcome the bias to suggest the occurrence of a damage scenario. Hence, in order to account for the evidence of a damage state, the co-variance of the prior distribution is assumed as known, while the mean value μ is updated step by step. In such a way, the posterior distribution at time t can give information on which value of damage-sensitive parameter is more plausible or believable, given the evidence of new data $\mathbf{d}(t)$. Moreover, assuming that the identified model parameters k_j are statistically independent [47, 30], they are separately updated over time and Eq. (9) can be rewritten as follows:

$$p(k_j|\mathbf{d}, t) = c \cdot p(\mathbf{d}|k_j, t) \cdot p(k_j|\mu(t-1)) \tag{10}$$

where the likelihood function $p(\mathbf{d}|k_j, t)$ is modeled as a Gaussian distribution with zero mean:

$$p(\mathbf{d}|k_j, t) = \frac{1}{\left[2\pi \prod_{i=1}^{M} (\sigma_{f_i}\sigma_{\Phi_i})^2\right]^{(MD)/2}} \exp\left(-\frac{1}{2}\sum_{m=1}^{D}\sum_{i=1}^{M} J_i^{\mathrm{err}}(k_j, d_k, t)\right) \tag{11}$$

where index $i = 1, .., M$ refers to the reference parameter associated to the i^{th} vibration mode; index $m = 1, .., D$ represents the number of measured data collected in vector $\mathbf{d}$; J_i^{err} is a fit function (error function) which quantifies the discrepancy between the experimental data and the FE model results at time t and it can be written as:

$$J_i^{\mathrm{err}} = (\sigma_{f_i})^{-2} e_{f_i}^2(x_j, \mathbf{d}) + (\sigma_{\Phi_i})^{-2} e_{\Phi_i}(x_j, \mathbf{d}); \tag{12}$$

where:

$$e_{f_i} = f_i^{\exp} - \hat{f}_i(x_j)) \tag{13}$$

$$e_{\mathbf{\Phi}_i} = \left(\mathbf{\Phi}_i^{\exp} - a_i\hat{\mathbf{\Phi}}_i(x_j)\right)^T\left(\mathbf{\Phi}_i^{\exp} - a_i\hat{\mathbf{\Phi}}_i(x_j)\right), \tag{14}$$

with $a_i = \left(\mathbf{\Phi}_{i,\exp}^T\hat{\mathbf{\Phi}}_i(x_j)\right)/\left(\hat{\mathbf{\Phi}}_i^T(x_j)\hat{\mathbf{\Phi}}_i(x_j)\right)$ mode shape scaling factor; σ_{f_i}, σ_{Φ_i} being the standard deviations associated to the ith natural frequency and mode shape which can be arbitrarily assumed or evaluated on the basis of the statistical measures [47]. For the sake of clarity, in the present application σ_{f_i} and σ_{Φ_i} are directly evaluated on the basis of statistical measures on the available data with the main objective of reducing the computational effort. It is worthwhile to underline that a better quantification of the likelihood function might lead to a more accurate estimation of the posterior distribution, which is an aspect that will deserve a special attention in future developments of this work.

2.5. Probabilistic damage identification

The Bayesian model updating is extended to be used for the probabilistic damage identification. In particular, according to [30, 48], the probability P_j^{dam} that the updated jth parameter k_j^{up} in a possibly damaged state is reduced from the undamaged state k_j^{ref} can be written as:

$$P_j^{\text{dam}} = P\left(k_j^{\text{up}} \leqslant (1-\overline{k}_j)k_j^{\text{ref}}|\mathbf{d}^{\text{ref}}, \mathbf{d}^{\text{dam}}\right) = F\left(\frac{(1-\overline{k})k_j^{\text{ref}} - k_j^{\text{up}}}{\sqrt{(1-\overline{k})^2\sigma_{k_j^{\text{ref}}}^2 + \sigma_{k_j^{\text{up}}}^2}}\right) \tag{15}$$

where $F(\cdot)$ is the standard Gaussian cumulative distribution function, $\overline{k}_j \in [0.1]$ is a damage threshold selected for the jth damage scenario and $k_j^{ref} = 1$ is the reference undamaged state. Changes in P_j^{dam} are studied as a sign of possible damage. The case of $k_j^{\text{up}} = (1-\overline{k}_j)k_j^{\text{ref}}$ leads to $P_j^{\text{dam}} = 0.5$ which is defined as alarm function P_j^{al}, meaning that the the damage threshold hypothesized for the jth damage scenario is reached. The case of $k_j^{\text{up}} > (1-\overline{k}_j)k_j^{\text{ref}}$ leads to $P_j^{\text{dam}} < 0.5$, denoting that the damage threshold is not reached. Finally,

the case of $k_j^{\mathrm{up}} < (1 - \overline{k}_j)k_j^{\mathrm{ref}}$ leads to $P_j^{\mathrm{dam}} > 0.5$, revealing that the damage threshold is exceeded.

Additionally, in order to clearly define a possible damage state, a damage factor DF can be introduced as:

$$DF = \frac{k_j^{ref} - k_j^{up}}{\overline{k}_j} \tag{16}$$

From Eq. (16) it is possible to obtain DF=0 if $k_j^{up} = k_j^{ref}$ and DF=1 if $k_j^{ref} - k_j^{up} = \overline{k}_j$. If DF>1, it means that k_j^{up} is strongly reduced with respect to the threshold $\overline{k}_j$. DF increases as $\overline{k}_j$ tends to zero, meaning that the modal modification extracted from the data probably doesn't correspond to the jth damage scenario (possible false alarm).

3. The case study

The Consoli Palace is a medieval building located in Gubbio, Umbria, central Italy, which dates back to the 14th century. The complexity of the building lies in the articulated internal distribution of volumes and materials. Globally, the structure has a rectangular plan and it is arranged on a series of floors above (about 60 meters) and under (about 10 meters) the square level. With reference to Fig. 3, three structural components can be identified: a central body; a loggia, connected to the main structure along the south wall; a bell tower. The architectural style of each façade (East and West side), is characterized by round arched windows and merlons in the rooftop. The load-bearing walls have a thickness of about 1.2 m and they are connected through horizontal masonry vaults. The Palace is built in calcareous stone masonry with a regular and homogeneous texture.

3.1. The continuous SHM system

The monitoring system (Fig. 3) was installed by the Department of Civil and Environmental Engineering of University of Perugia in July 2020 within the

framework of the PRIN2017 detect aging project (cfr. Acknowledgments) and it is characterized by:

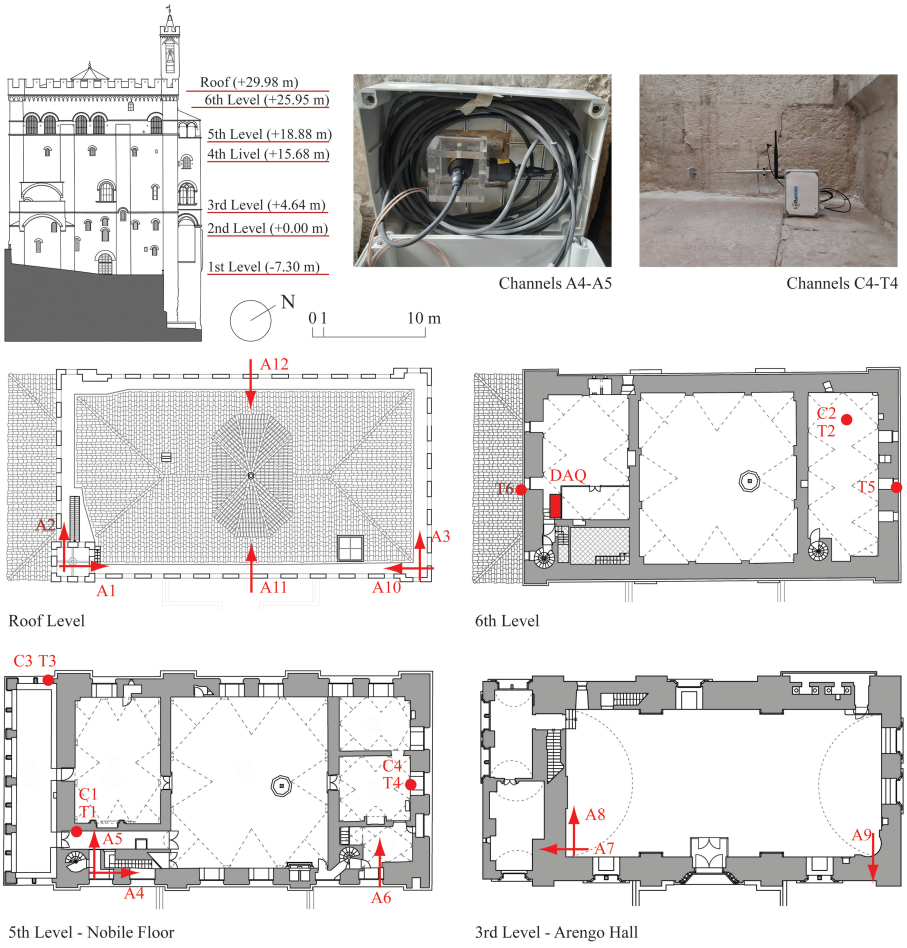

Figure 3: Continuous monitoring configuration.differenziare rispetto a figura CSHM. NICOLA

- a data acquisition system;
- twelve unidirectional accelerometers A1-A12, model PCB393B12 (measurement range $\pm$ 0.5 g, frequency range 0.15-1000 Hz, broadband resolution 8 μg, resonant frequency $\geq$ 10 kHz) installed at the 3rd, 5th and roof level;
- four S-series linear variable transducers (LVDTs), denoted as C1-C4 (mea-

surement range 0-0.5 mm, resolution 0.31 m);

- four K-type thermocouples;
- a wiring system connecting the sensors to a NI CompactDAQ-9132 data acquisition system equipped with a NI 9234 acquisition module for accelerometers (24-bit resolution, 102-dB dynamic range, and anti-aliasing filters) and a NI 9219 acquisition module (24-bit resolution, +-60 V range, 100 S/s) for LVDTs and thermocouples.

The monitoring system was activated on July 18th 2020. Table 1 summarizes the SHM sensors' network. Acceleration data are stored in separate files containing 30 min-long recordings with a sampling frequency of 100 Hz, while crack amplitudes and temperature values are sampled at 0.1 Hz. Data are transferred and contained in a cloud storage, and can be accessed by system administrators and visualized in a web-based platform.

The frequency tracking during the time period July 18th 2020 - December 20th 2021 is depicted in Fig. 4 a) with the indication of the selected training period. Fig. 4 b) shows the tracking of the MAC value and Fig. 4 c) of the Modal Phase Collinearity (MPC) index, which expresses the linear functional relationship between the real and the imaginary parts of the unscaled mode shape vectors. The high values of the MPC index confirm the presence of real normal modes.

3.2. FE model

In order to reproduce the structural dynamic behaviour (local and global vibration modes) identified throught Ambient Vibration Tets (AVT), a 3D FE model of the structure has been built and calibrated within the Abaqus environment [49], as detailed in [13]. The mesh of the masonry is composed by three-dimensional tetrahedral and hexahedral first-order elements. An isotropic material is assigned to the FE model with invariant properties under rotation of each axis. Since masonry can be considered as a quasi-brittle material whose mechanical performance deteriorates (softens) under monotonic or cyclic loading, the non-linear behavior of the material is reproduced by using the well

Channel	Level	Measure	Direction
A1	rooftop	acceleration	y
A2	rooftop	acceleration	x
A3	rooftop	acceleration	y
A4	5	acceleration	y
A5	5	acceleration	x
A6	5	acceleration	y
A7	3	acceleration	$-y$
A8	3	acceleration	x
A9	3	acceleration	$-x$
A10	rooftop	acceleration	$-y$
A11	rooftop	acceleration	x
A12	rooftop	acceleration	$-x$
C1-C3-C4	5	crack's length	–
C2	6	crack's length	–
T2	6	temperature	–
T1-T3-T4	5	temperature	–

Table 1: SHM sensors' network within the building.

known concrete damage plasticity (CDP) model, introduced by [50, 51]. Indeed, the CDP model is particularly suitable for masonry structures in which the material is particularly prone to damage [52]. The non-linear constitutive law takes into consideration the degradation of the elastic stiffness induced by plastic straining both in tension and compression. According to [53], in order to describe the inelastic multi-dimensional behavior, masonry is modeled through the Drucker-Prager strength criterion with $K_c = 0.667$, which represents the shape of the yield surface in plane stress ($K_c = 1$ stands for a circular surface); a value equal to 0.1 is adopted for the eccentricity term; the dilatancy angle is assumed equal to 10°; the ratio between the ultimate compression strength in biaxial stress states and in uniaxial conditions is set equal to 1.16; the viscosity

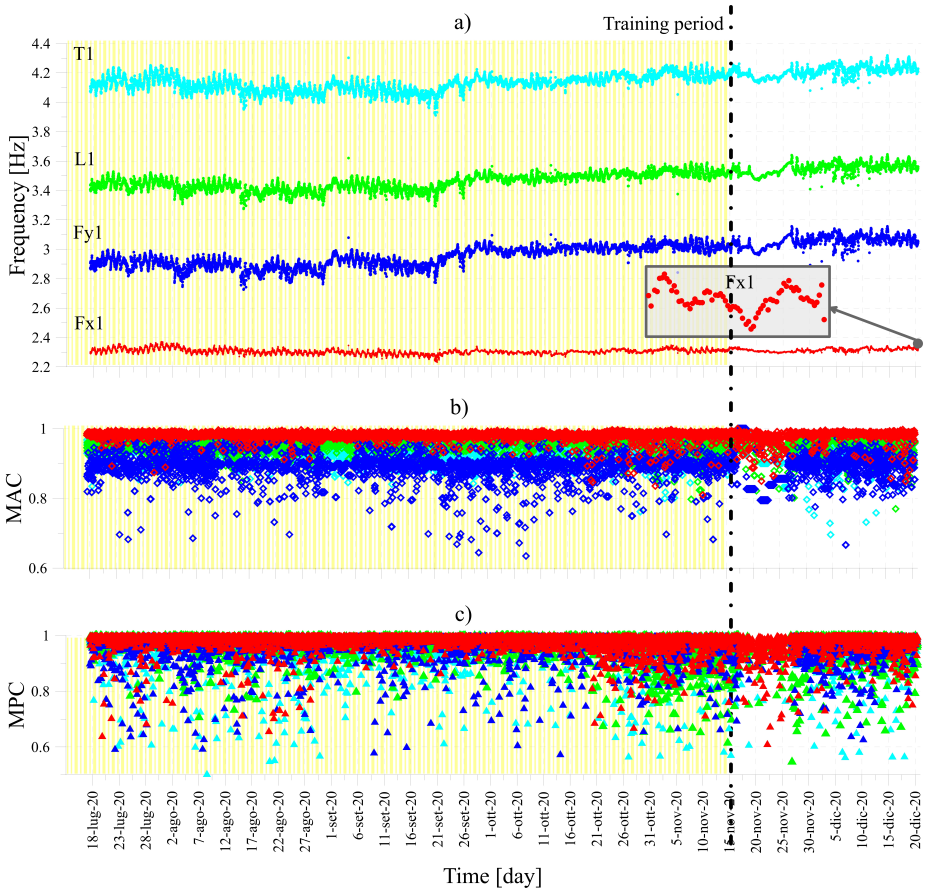

Figure 4: MF tracking during the time period July 18th 2020 - December 20th 2021: a) Frequency tracking; b) MAC tracking; c) MPC tracking.

parameter is assumed equal to 0.002.

As reported in Fig. 5, four vibration modes are selected for the numerical simulations:

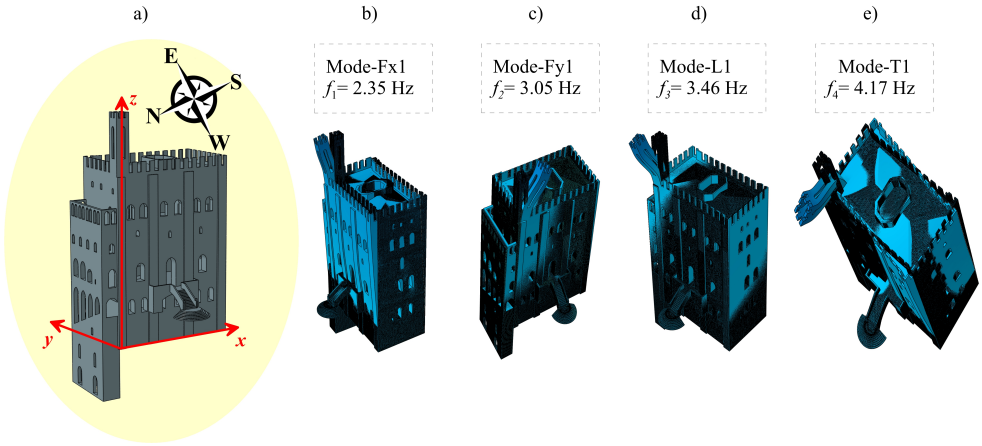

Figure 5: Principal vibration modes: a) Fx1; b) Fy1; c) L1; d) T1.

- Fx1: global flexural mode along the East-West direction (f_1=2.35 Hz and MAC=0.98);
- Fy1: global flexural mode along the North-South direction direction (f_2=3.05 Hz and MAC=0.76);
- L1: local mode which pertains to the bell tower (f_3=3.46 Hz and MAC=0.64)
- T1: global torsional mode (f_4=4.17 Hz MAC=0.97).

The relatively low agreement between experimental and numerical higher order mode shapes was already discussed in [13, 54].

3.3. Selection of damage scenarios

NLSA along the two main directions of the building are carried out in order to identify potential cracking patterns that can be activated by an earthquake, and associate such patterns to damage-prone regions. As a matter of fact, some of the cracks already existing in the palace (e.g. the crack vertically oriented along the south wall) agree with the numerically predicted cracking patterns, indicating that some of the damaging mechanisms are already activated.

More in detail, NLSA allows to determine two damage scenarios (Fig. 6b-c): D2 which represents the crack pattern resulting from NLSA along x direction

capable of reproducing the existing pattern, especially along the south wall Fig. 6b) and the internal horizontal vaults; D3 which refers to the crack pattern resulting from NLSA along the y direction 6c).

Furthermore, on the basis of the Engineering judgment, additional damage-

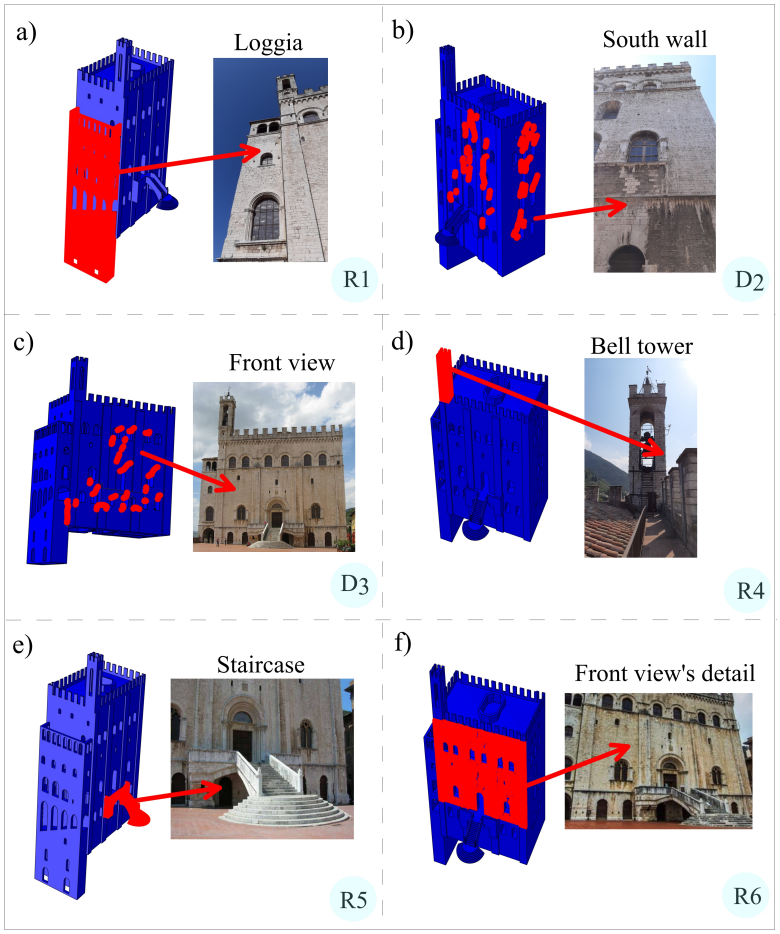

Figure 6: Selected damage sensitive areas with reference to both FE model and real structure: a) R1, the loggia; b) D2, crack pattern y; c) D3, crack pattern x, d) R4, the bell tower; e) R5, the staircase; f) R6, the façade degradation.

350

prone regions are selected: R1, which represents the poor connection exerted between the loggia and the central body of the Consoli Palace; R4, which refers to the bell tower (Fig. 6d); R5, which represents damage to the principal

staircase (Fig.6e); R6, which represent degradation of the exterior texture of the main façade of the building, i.e., West façade (Fig.6c). In such areas, the Young's modulus of the isotropic material is assumed as uncertain. Hence, the vector collecting the uncertain parameters is $\mathbf{X} = \{k_1, .., k_6\}$.

4. Analysis results

4.1. Simulation-based damage scenarios

In order to calibrate the surrogate model, a total number of 500 samples (N_s) are randomly simulated for the uncertain parameters collected in vector $\mathbf{X}$. Figs. 7 a)-d) illustrate the correspondence of both frequencies (R^2) and

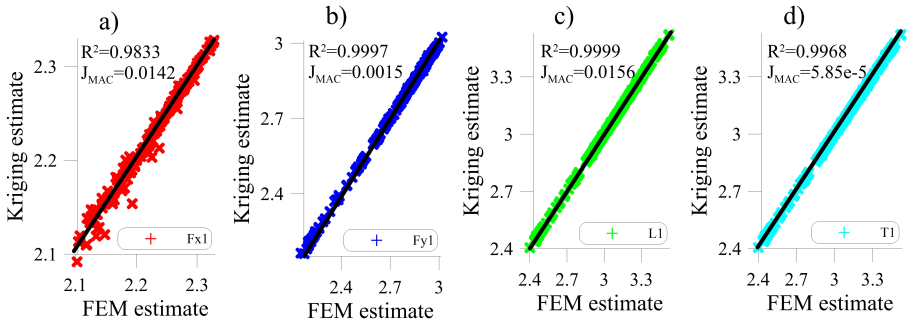

Figure 7: FEM estimate vs Kriging estimate for the selected principal vibration modes: a) samples of mode Fx1 ; f) samples of mode Fy1 ; g) samples of mode L1 ; h) samples of mode T1.

mode shapes $\left(\mathrm{J_{MAC}} = 1/N_s \sum_i (1 - MAC_i)\right)$ evaluated from the FE model and the Kriging model. From the figure it can be noted that the surrogate predicted frequencies and mode shapes (Kriging estimate) well fit the corresponding FE values.

The DT-based sensitivity damage chart SDC relating frequencies and uncertain parameters is depicted in Fig. 8, which enables to associate the expected value of k_j, i.e. the reduction of the jth stiffness of the masonry, to a defined frequency decay.

A graphical representation of the frequencies which mostly affect the damage

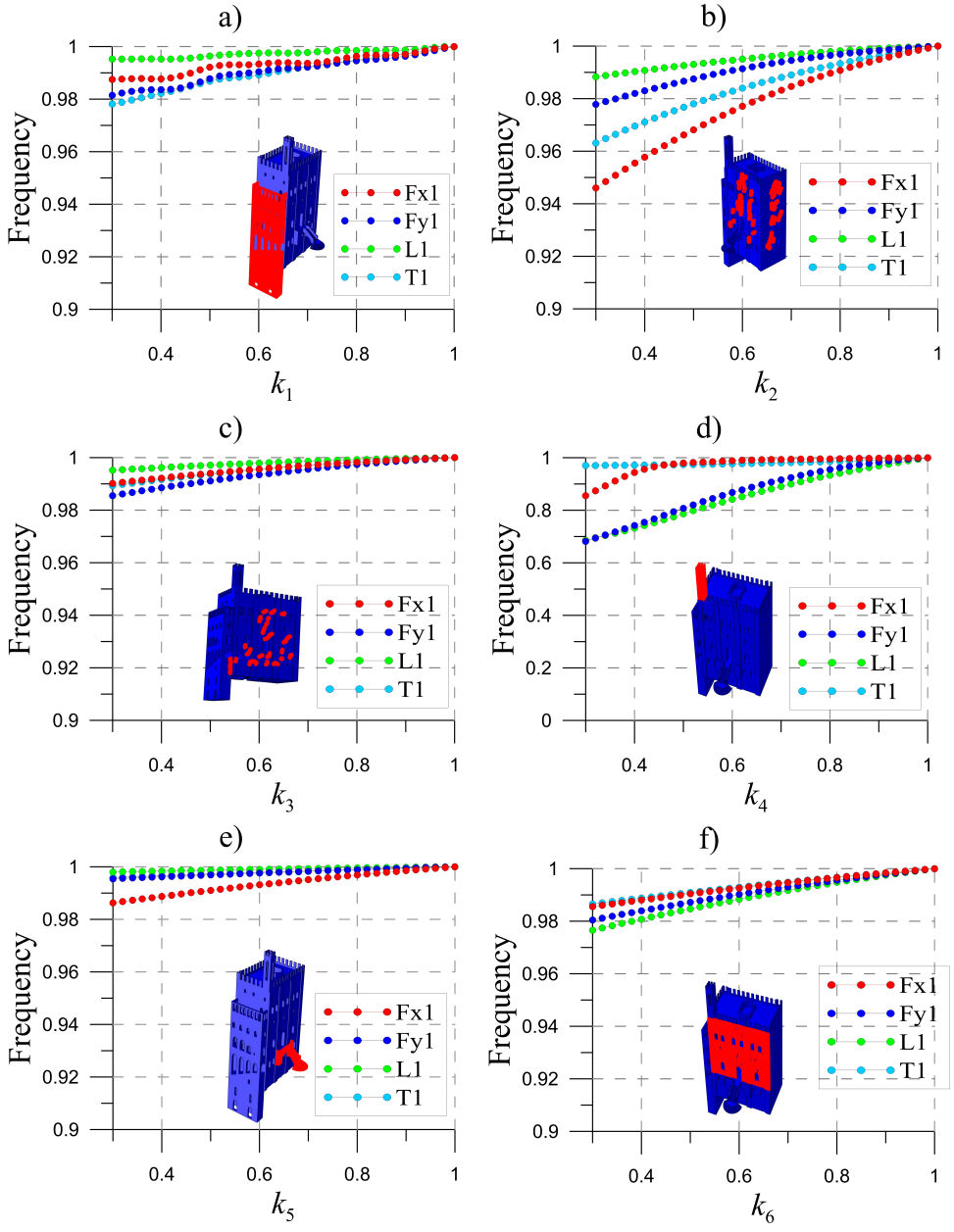

Figure 8: SDC for frequencies decays: a) D1; b) D2; c) D3; d) D4; e) D5; f) D6.

occurrence for each damage scenario is illustrated in Table 2. Indeed, due to the observed frequency decay, Fx1 (flexural mode along the x direction) appears as the most damage-sensitive vibration mode for damage scenarios D2 and D5, Fy1 (flexural mode along the y direction) for D1, D3, D4 and D6, L1 (local mode which pertains to the bell tower) for D4 and D6, and T1 (torsional mode) for D1 and D2.

It is worth noticing that small variations can daily occur in the frequency tracking and, even if environmental effects are removed, a frequency decay smaller than 1% can be considered as negligible.

The DT-based sensitivity damage chart SDC, which relates MAC values and

Mode shape	D_1	D_2	D_3	D_4	D_5	D_6
Fx1		■			■	
Fy1	■		■	■		■
L1				■		■
T1	■	■				

Table 2: Sensitivity table of frequency decay for $k_j = 0.3$.

uncertain parameters, is depicted in Fig. 9. From the figure it can be observed that MAC variations can be considered negligible (equal or less than 1 %) for all damage scenarios except for D1 and D4. Indeed, a reduction of k_1 provokes a modification in the local L1 mode shapes and a reduction of k_4 induces a huge reduction of Fy1 and L1 MAC values.

4.2. Bayesian model updating

This section summarizes the main results of the Bayesian model updating. Uncertain parameters are updated once the model is trained, i.e, starting from November 15^{th} 2020. From that moment on, the monitored data are gathered together in subgroups of daily components (t) in order to perform the Bayesian model updating continuously over time on a daily basis. The first 20 days are

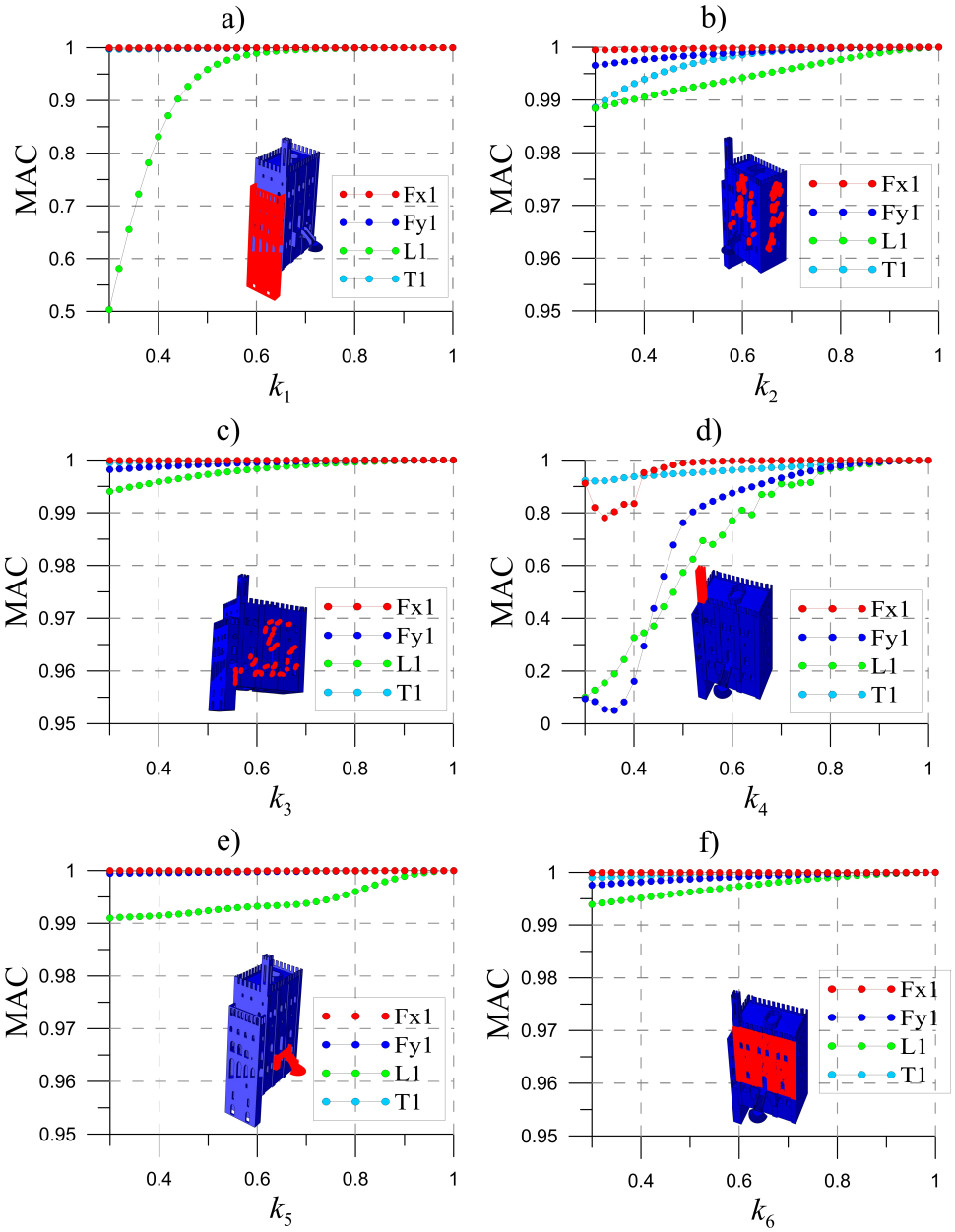

Figure 9: SDC for MAC decays: a) D1; b) D2; c) D3; d) D4; e) D5; f) D6.

considered as undamaged, then a damage scenario is simulated and the frequency of the model updating is incremented on hourly basis (t^*), according to Sect 2.

Fig. 10 illustrates the posterior distributions associated to the uncertain pa-

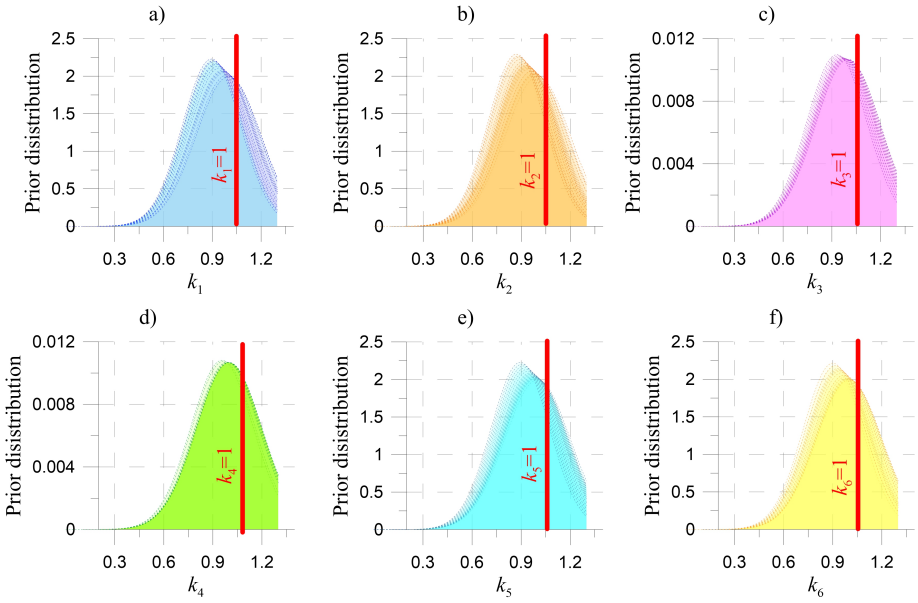

Figure 10: Bayesian-based prior distributions (undamaged structure) as a function of k_j: a) R1; b) D2; c) D3; d) R4; e) R5; f) R6.

rameters $k_1, .., k_6$ among the undamaged time period. With reference to the figure, a fluctuation of the mean value of k_j between about 0.9 and 1 can be observed. This result can be related to the fact that the reference SDC is sensitive to the slight variations which can daily occur in the frequency and MAC tracking and to the initial FE modeling errors. It is worth mentioning that the sensitivity to changing environmental conditions can be considerably reduced by considering an appropriate training period, i.e. 1 year.

Figure 11 illustrates the comparison between DF, P^{dam} and k_j^{up} over the number of updates, when simulating the occurrence of damage scenario D2, extrapolated from the damage sensitivity chart in correspondence with $k_2 = 0.3$ (Fig. 8b). According to the damage chart, the values of the frequency decays are: i) d=0.04

for Fx1; ii) d=0.01 for Fy1; iii) d=0.01 for L1; iv) d=0.03 for T1.

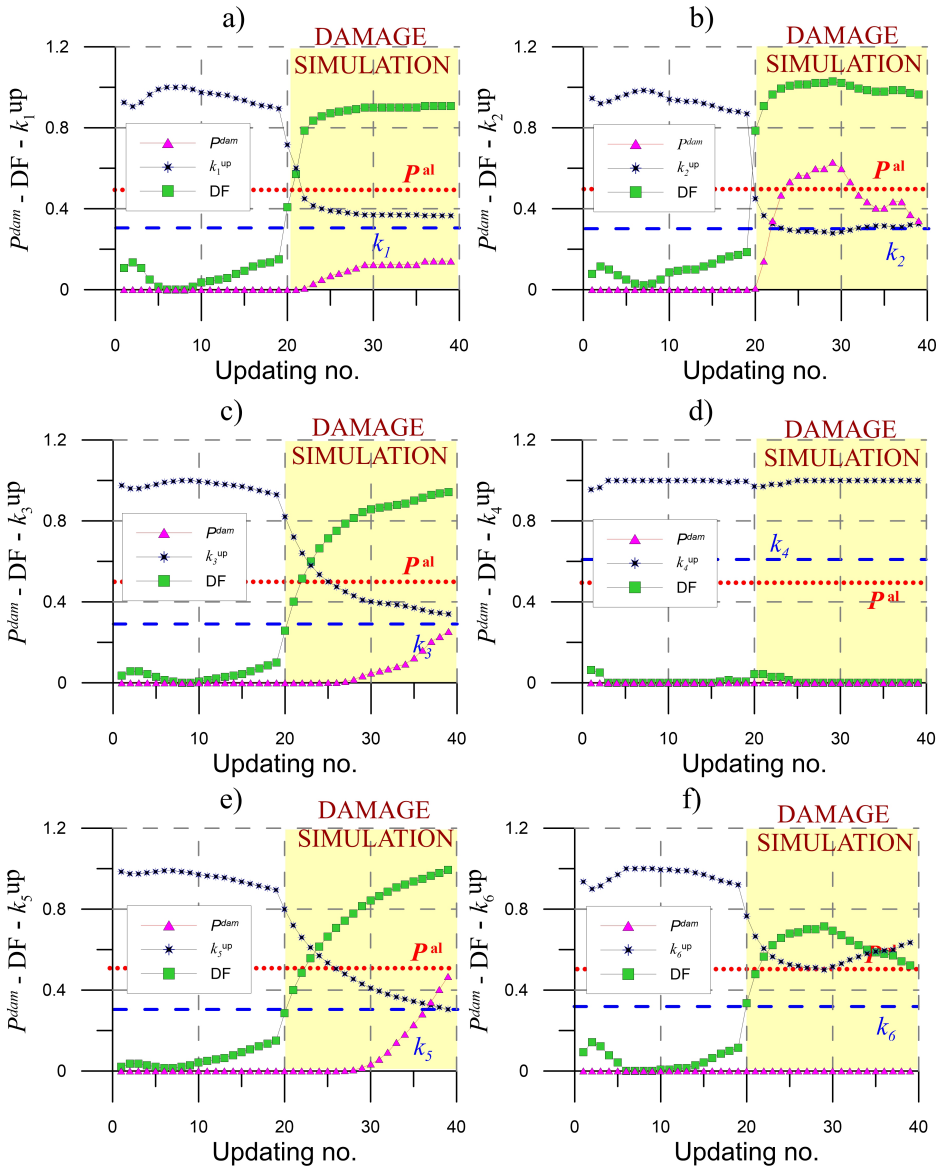

Figure 11: Comparison between DF, P^{dam} and k^{up} over the number of updates by simulating the occurrence of D2 for $k_2 = 0.3$ for each damage scenario with the indication of P^{al} and $\overline{k}_j$: a) D1 $\overline{k}_1 = 0.3$; b) D2 $\overline{k}_2 = 0.3$; c) D3 $\overline{k}_3 = 0.3$; d) D4 $\overline{k}_4 = 0.6$; e) D5 $\overline{k}_5 = 0.3$; f) D6 $\overline{k}_6 = 0.3$.

The values of $\overline{k}_j$ are defined as follows: a) D1 $\overline{k}_1 = 0.7$; b) D2 $\overline{k}_2 = 0.7$; c) D3 $\overline{k}_3 = 0.7$; d) D4 $\overline{k}_4 = 0.4$; e) D5 $\overline{k}_5 = 0.7$; f) D6 $\overline{k}_6 = 0.7$. Since D4 pertains to the bell tower, a reduction of the bell tower's stiffness corresponding to 40 % ($k_4 = 0.6$) is considered adequate as a reference damaged state. From the Figure it can be noted that P^{al} is reached for scenario D2, as expected, and for scenario D5. This result, consistently with Table 2, means that, due to the frequency decay of mode Fx1, both damage scenarios D2-D5 can be designated to damage. The case of D5 deserves a particular attention, since P^{dam} tends to 1 and DF approaches 1 (k_5^{up} approaches $\overline{k}_5$) and needs to be checked in the real-world structure in order to avoid a false alarm (see Sect 2.5). On the contrary, the remaining damage scenarios have a smaller probability of occurrence.

For the sake of brevity, results in terms of prior and posterior distributions for only damage scenarios D2 and D4, when the damage scenario D2 is simulated are depicted in Figs. 12a) (D2) and b) (D4). From the results it can be observed that, consistently with the SDC, the simulated damage scenario barely affects k_4 in the damaged state (Fig. 12b), since the mean value of the posterior distribution doesn't significantly change between healthy and damaged condition. Nevertheless, Fig. 12a) highlights the evolution of the posterior distributions in comparison with the prior distributions of k_2 at each update. Consistently with the SDC (Fig. 8), in the healthy status the updated distributions are grouped around higher values of k_2 while the occurrence of damage is clearly highlighted by a translation of the posterior curves towards reduced values of the selected uncertain parameter. In detail, it can be observed that the Bayesian-based procedure is able to correctly account for the frequency decays tracing back to the simulated damage scenario D2, i.e., $k_2 \approx 0.3$.

For completeness, the results in terms of DF and P^{dam} for a damage scenarios characterized by both a significant and a slight frequency decay (D4 and D6) are shown in Figs. 13a)-n). According to the damage chart the values of the frequency decays for D4 and D6 corresponding to $k_4 = 0.6$ and $k_6 = 0.3$ are summarized in Table 3. Moreover, in the case of D4, the MAC decays are defined as (Fig. 9d): 0.89 for Fy1; 0.8 for L1; 0.98 for T1.

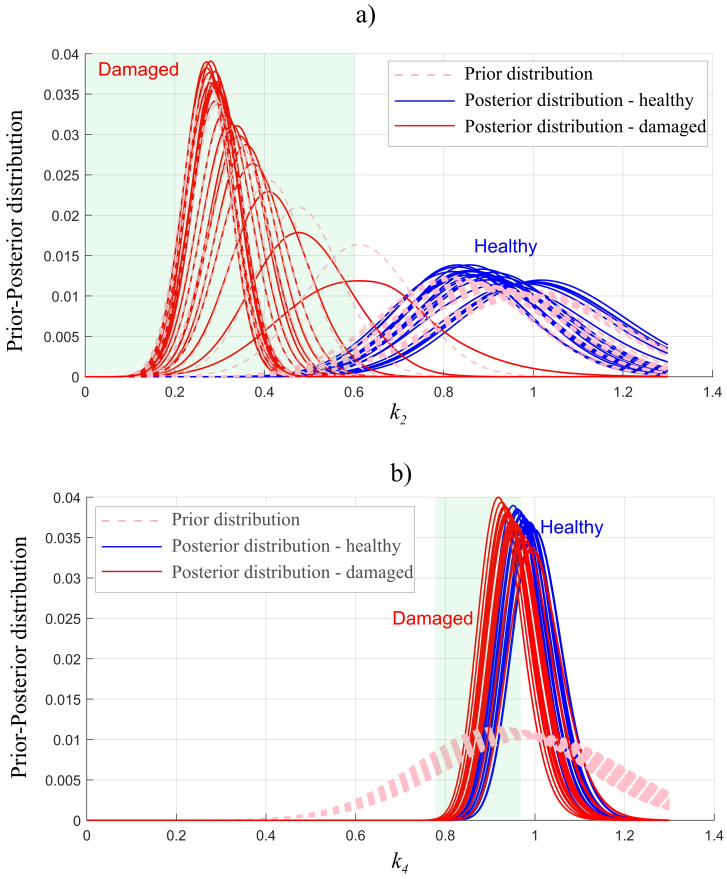

Figure 12: Bayesian-based prior and posterior distributions by simulating damage scenario D2 for $k_2 = 0.3$: a) D2; b) R4.

Damage scenario	Fx1	Fy1	L1	T1
D4	0.03	0.13	0.15	0.03
D6	0.00	0.01	0.01	0.02

Table 3: Frequency decays (%) d for damage scenarios D4 with $k_4 = 0.6$ and damage scenario D6 with $k_6 = 0.3$.

From the figure it can be noted that the simulation of D4 induces an increase of P^{dam} for D1, D2, D3, and D6 with values approximately equal to 1 and values of DF strongly higher than 1 (green area), meaning that the updated k^{up} values tends to zero, highlighting the possibility of a false alarm being detected. The damage scenario D5, whose triggering does not depend on Fy1

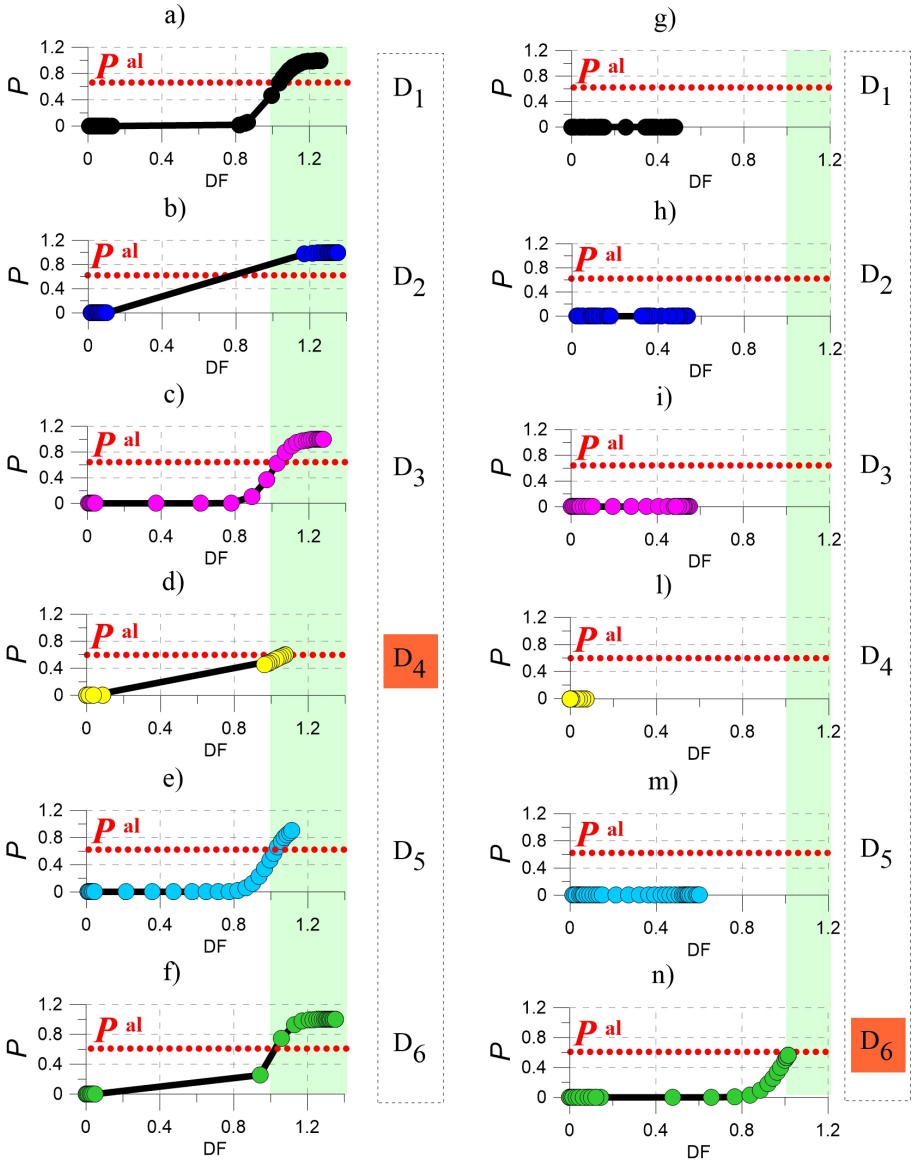

Figure 13: DF versus P^{dam} by simulating damage scenarios D4 and D6: a)-f) damage scenarios D1-D6 by simulating D4; g)-n) damage scenarios D1-D6 by simulating D6.

and L1, reaches P^{al} after a certain number of updates (see the multiple points in damaged area). This fact is due to the higher sensitivity of D5 to small variations associated to Fx1. This sensitivity can be reduced by means of an efficient removal of environmental effects that will be reached after 1 year of

training period. Moreover, the damage scenario D4 perfectly fits the simulated one. Indeed, it is clearly visible the occurrence of the damaged state, since P^{dam} reaches 0.5 and DF reaches 1 immediately at the first step of model updating. Finally, Figs. 13 g)-n) demonstrate that a damage scenario (D6) associated with a slight frequency decay, allows to keep out D1-D2-D3-D4-D5, and suggests to pay specific attention to those damage scenarios associated with smaller frequencies variations.

5. Conclusions

The present paper has presented a transfer learning Bayesian methodology for structural health monitoring of monumental buildings. The proposed method enters in the challenging context of integrated SHM, consisting of a permanent network of sensors installed in historical buildings capable of assessing continuously over time the structural condition.

The main advantages and innovations of the proposed approach concern the use of real-time long-term monitoring data, the robust identification of possible damage scenarios by using the TL concepts, where a digital twin allows to transfer knowledge between numerical models and monitoring data and the use of damage probabilities, which allow an essential support for decision making.

The case study is the Consoli Palace, located in Umbria (Italy), which has been monitored since 2015 with an improvement of the SHM sensors' network in 2020. The data stored between July 18$^{\mathrm{th}}$ 2020 and January 14$^{\mathrm{th}}$ 2021 have been used for the analysis. A FE model able to reproduce the identified structural dynamic behavior has been built and a series of NLSA, in conjunction with Engineering judgment, enabled to select damage-sensitive portions of the structure. A DT of the structure has been calibrated by using the Kriging model in order to define the SDC as a prior knowledge of possible damage. Then, a real time Bayesian model updating of the selected uncertain parameters has been performed in order to continuously identify the probability of damage occurrence. For the purpose, different damage scenarios have been artificially simulated by select-

ing appropriate frequency decays from the SDC. As confirmed by the results, the proposed approach is able to consistently check any variation of the structural condition in a probabilistic manner by appropriately considering long term monitoring data. The use of damage factors and damage probabilities allow to identify possible false alarms.

Ackowledgments

The Authors would like to acknowledge the support of the PRIN 2017 project, "DETECT-AGING" (Prot. 201747y73L).

References

[1] C. Farrar, K. Worden, An introduction to structural health monitoring, Philosophical Transactions of the Royal Society A 365 (1851) (2007) 303–315. doi:10.1098/rsta.2006.1928.

[2] F. Parisi, N. Augenti, Earthquake damages to cultural heritage constructions and simplified assessment of artworks, Engineering Failure Analysis 34 (2013) 735 – 760.

[3] Y. Kaya, E. Safak, Real-time analysis and interpretation of continuous data from structural health monitoring (shm) systems, Bulletin of Earthquake Engineering 13 (3) (2015) 917–934.

[4] N. Cavalagli, G. Comanducci, F. Ubertini, Earthquake-induced damage detection in a monumental masonry bell-tower using long-term dynamic monitoring data, Journal of Earthquake Engineering 22 (supl) (2018) 96–119.

[5] A. Downey, A. D'Alessandro, S. Laflamme, F. Ubertini, Smart bricks for strain sensing and crack detection in masonry structures, Smart Materials and Structures 27 (1).

[6] I. Venanzi, A. Kita, N. Cavalagli, L. Ierimonti, F. Ubertini, Earthquake-induced damage localization in an historic masonry tower through long-term dynamic monitoring and fe model calibration, Bulletin of Earthquake Engineering 18 (5) (2020) 224–2274.

[7] S. Bennati, L. Nardini, W. Salvatore, Dynamic behaviour of a medieval masonry bell tower. ii. measurement and modelling of the tower motion, Journal of Structural Engineering 131 (2005) 1656–1664.

[8] S. Ivorra, F. Pallarés, Dynamic investigations on a masonry bell tower, Engineering Structures 28 (5) (2006) 660 – 667.

[9] L. Ramos, L. Marques, P. Lourenco, G. De Roeck, A. Campos-Costa, J. Roque, Monitoring historical masonry structures with operational modal analysis: two case studies., Mechanical Systems and Signal Processing 24 (2010) 1291–1305.

[10] C. Gentile, A. Saisi, A. Cabboi, Structural identification of a masonry tower based on operational modal analysis, International Journal of Architectural Heritage 9 (2) (2015) 98–110.

[11] F. Ubertini, N. Cavalagli, A. Kita, G. Comanducci, Assessment of a monumental masonry bell-tower after 2016 central italy seismic sequence by long-term shm, Bulletin of Earthquake Engineering 16 (2018) 775–801.

[12] F. Ubertini, G. Comanducci, N. Cavalagli, A. Pisello, A. Materazzi, F. Cotana, Environmental effects on natural frequencies of the san pietro bell tower in perugia, italy, and their removal for structural performance assessment, Mechanical Systems and Signal Processing 82 (2017) 307–322.

[13] A. Kita, N. Cavalagli, F. Ubertini, Temperature effects on static and dynamic behavior of consoli palace in gubbio, italy, Mechanical Systems and Signal Processing 120 (2019) 180–202.

[14] E. García-Macías, L. Ierimonti, I. Venanzi, F. Ubertini, An innovative methodology for online surrogate-based model updating of historic buildings using monitoring data, International Journal of Architectural Heritage.

[15] E. García-Macías, L. Ierimonti, I. Venanzi, F. Ubertini, Comparison of surrogate models for handling uncertainties in shm of historic buildings, Lecture Notes in Mechanical Engineering (2020) 1645–1657.

[16] A. Cury, C. Cremona, Assignment of structural behaviours in long-term monitoring: Application to a strengthened railway bridge., Structural Health Monitoring 11 (2012) 422–441.

[17] F. Ubertini, G. Carmelo, A. Materazzi, Automated modal identification in operational conditions and its application to bridges, Engineering Structures 46 (2013) 264–278.

[18] L. Sun, Z. Shang, Y. Xia, S. Bhowmick, S. Nagarajaiah, Review of bridge structural health monitoring aided by big data and artificial intelligence: From condition assessment to damage detection, Journal of Structural Engineering (United States) 146 (5).

[19] A. Cancelli, S. Laflamme, A. Alipour, S. Sritharan, F. Ubertini, Vibration-based damage localization and quantification in a pretensioned concrete girder using stochastic subspace identification and particle swarm model updating, Structural Health Monitoring 19 (2) (2020) 587–605.

[20] D. Tibaduiza Burgos, R. Gomez Vargas, C. Pedraza, D. Agis, F. Pozo, Damage identification in structural health monitoring: A brief review from its implementation to the use of data-driven applications, Sensors (Switzerland) 20 (3).

[21] E. Simoen, G. De Roeck, G. Lombaert, Dealing with uncertainty in model updating for damage assessment: A review, Mechanical Systems and Signal Processing 56-57 (2015) 123–149.

[22] K.-V. Yuen, L. Katafygiotis, Bayesian time-domain approach for modal updating using ambient data, Probabilistic Engineering Mechanics 16 (3) (2001) 219–231.

[23] S.-K. Au, Uncertainty law in ambient modal identificationpart i: Theory, Mechanical Systems and Signal Processing 48 (1-2) (2014) 15–33.

[24] S.-K. Au, Uncertainty law in ambient modal identification-part ii: Implication and field verification, Mechanical Systems and Signal Processing 48 (1-2) (2014) 34–48.

[25] W.-J. Yan, L. Katafygiotis, An analytical investigation into the propagation properties ofuncertainty in a two-stage fast bayesian spectral densityapproach for ambient modal analysis, Mechanical Systems and Signal Processing 118 (2019) 503–533.

[26] W.-J. Yan, L. Katafygiotis, A novel bayesian approach for structural model updating utilizing statistical modal information from multiple setups, Structural Safety 52 (PB) (2015) 260–271.

[27] C. Pepi, M. Gioffre', M.-D. Grigoriu, Parameters identification of cable stayed footbridges using bayesian inference, Meccanica 54 (9) (2019) 1403–1419.

[28] J. Beck, L. Katafygiotis, Updating models and their uncertainties. i: Bayesian statistical framework, Journal of Engineering Mechanics 124 (4) (1998) 455–461. doi:10.1061/(ASCE)0733-9399(1998)124:4(455).

[29] K. Yuen, Bayesian Methods for Structural Dynamics and Civil Engineering, John Wiley & Sons (Asia) Pte Ltd, 2 Clementi Loop, # 02-01, Singapore 129809, 2010.

[30] I. Behmanesh, B. Moaveni, G. Lombaert, C. Papadimitriou, Hierarchical bayesian model updating for structural identification, Mechanical Systems and Signal Processing 64–65 (2015) 360–376.

[31] I. Behmanesh, B. Moaveni, Accounting for environmental variability, modeling errors, and parameter estimation uncertainties in structural identification, Journal of Sound and Vibration 374 (2016) 92–110.

[32] H. Sun, A. Mordret, G. Prieto, M. Toksz, O. Bykztrk, Bayesian characterization of buildings using seismic interferometry on ambient vibrations, Mechanical Systems and Signal Processing 85 (2017) 468–486.

[33] R. Rocchetta, M. Broggi, Q. Huchet, E. Patelli, On-line bayesian model updating for structural health monitoring, Mechanical Systems and Signal Processing 103 (2018) 174–195. doi:10.1016/j.ymssp.2017.10.015.

[34] G. Bartoli, M. Betti, A. Marra, S. Monchetti, A bayesian model updating framework for robust seismic fragility analysis of non-isolated historic masonry towers, Philosophical Transactions of the Royal Society A: Mathematical, Physical and Engineering Sciences 377 (2155).

[35] L. Ierimonti, I. Venanzi, N. Cavalagli, F. Comodini, F. Ubertini, An innovative continuous bayesian model updating method for base-isolated rc buildings using vibration monitoring data, Mechanical Systems and Signal Processing 139.

[36] C. Farrar, K. Worden, Structural Health Monitoring: A Machine Learning Perspective, 2012, john Wiley & Sons, Ltd. doi:10.1002/9781118443118.

[37] L. Rosafalco, A. Manzoni, S. Mariani, A. Corigliano, Fully convolutional networks for structural health monitoring through multivariate time series classification, Advanced Modeling and Simulation in Engineering Sciences 7 (1).

[38] A. Neves, I. Gonzlez, J. Leander, R. Karoumi, Structural health monitoring of bridges: a model-free ann-based approach to damage detection, Journal of Civil Structural Health Monitoring 7 (5) (2017) 689–702.

[39] A. Neves, I. González, J. Leander, R. Karoumi, A new approach to damage detection in bridges using machine learning, Lecture Notes in Civil Engineering 5 (2018) 73–84.

[40] L. Bull, T. Rogers, C. Wickramarachchi, E. Cross, K. Worden, N. Dervilis, Probabilistic active learning: An online framework for structural health monitoring, Mechanical Systems and Signal Processing 134 (2019) 106294.

[41] L. Bull, K. Worden, N. Dervilis, Towards semi-supervised and probabilistic classification in structural health monitoring, Mechanical Systems and Signal Processing 140 (2020) 106653.

[42] F. Schwenker, E. Trentin, Pattern classification and clustering: A review of partially supervised learning approaches, Pattern Recognition Letters 37 (1) (2014) 4–14.

[43] T. Rogers, K. Worden, R. Fuentes, N. Dervilis, U. Tygesen, E. Cross, A bayesian non-parametric clustering approach for semi-supervised structural health monitoring, Mechanical Systems and Signal Processing 119 (2019) 100–119.

[44] E. Garca-Macas, F. Ubertini, Mova/moss: Two integrated software solutions for comprehensive structural health monitoring of structures, Mechanical Systems and Signal Processing 143.

[45] R.-G.-D. Steel, J.-H. Torrie, Principles and Procedures of Statistics with Special Reference to the Biological Sciences, McGraw Hill, 1960.

[46] S. Lophaven, H. Nielsen, J. Søndergaard, A matlab kriging toolbox, version 2.0., Tech. Rep. IMM-TR-2002-12, Kongens Lyngby, Copenhagen, Denmark: Informatics and Mathematical Modelling, Technical University of Denmark, DTU. (2002).

[47] J. Jang, A. Smyth, Bayesian model updating of a full-scale finite element model with sensitivity-based clustering, Structural Control and Health Monitoring 24 (11).

[48] M. Vanik, L. Beck, S. Au, Bayesian Probabilistic Approach to Structural Health Monitoring, Journal of Engineering Mechanics 126 (7).

[49] c. Simulia, Abaqus Analysis User's Manual. Volume III: Materials, Dessault Systèmes, USA, 2010.

[50] J. Lubliner, J. Oliver, S. Oller, E. Oate, A plastic-damage model for concrete, International Journal of Solids and Structures 25 (3) (1989) 299–326.

[51] J. Lee, G. Fenves, Plastic-damage model for cyclic loading of concrete structures, Journal of Engineering Mechanics 124 (8) (1998) 892–900.

[52] M. Valente, G. Milani, Non-linear dynamic and static analyses on eight historical masonry towers in the north-east of italy, Engineering Structures 114 (2016) 241–270.

[53] G. Milani, M. Valente, C. Alessandri, The narthex of the church of the nativity in bethlehem: A non-linear finite element approach to predict the structural damage, Computers and Structures 207 (2018) 3–18.

[54] N. Cavalagli, A. Kita, V. Castaldo, A. Pisello, F. Ubertini, Hierarchical environmental risk mapping of material degradation in historic masonry buildings: An integrated approach considering climate change and structural damage, Construction and Building Materials 215 (2019) 998–1014.